A Modeling Study of Electrical Characteristics of Anisotropic Conductive Film Adhesives

Ranjith Divigalpitiya
3M Canada Laboratory
3M Canada Company. 1840 Oxford Street East. London. Ontario N5V 3R6 Canada
rdivigalpitiya@mmm.com

Abstract: Finite element analysis provides new insights into the electrical behaviour of conducting adhesives. We show that at a contact between a spherical conducting particle and a flat conducting substrate the current distribution is non-uniform: the current is concentrated at the periphery of the contact. In practice, the current concentration has important implications. We further shed light on what happens when a contact is contaminated with insulative debris. Finite element analysis and first principle calculations show that the contact resistance of coated particles is more immune to contaminants at the contact than solid metallic particles.

Keywords: conductive adhesives, contact resistance, electrical characteristics

1. Introduction

Anisotropic conductive film (ACF) adhesives are used in bonding circuit components both mechanically and electrically, in place of solder [1]. The light weight, lead-free materials, low cost, low application temperature, and ease of use are some of the reasons for the popularity of these adhesives. Essentially, ACFs are a mix of electrically conducting particles in an adhesive matrix; the adhesive bonds the parts mechanically while the conducting particles allow electrical connections to be made between the conducting pads or circuit traces as shown in cross-section in Figure. 1 in a typical application. The adhesive film is applied between the two parts to be bonded under some pressure, and depending on the adhesive, it may be heated at this step or exposed to UV etc., for curing it; the bonded pieces are then held by the cured adhesive under compressive stress. The adhesive maintains electrical contacts between the parts via conducting particles.
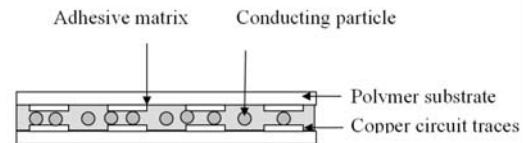

Figure. 1. A cross-sectional diagram of two circuit traces bonded with an ACF adhesive.

The electrical performance of ACFs has been studied in terms of their contact resistance [2 - 5]. Historically, the contact resistance of ACF has been modeled using the concept of constriction resistance (R_c) which relates to the diameter of the contact circle, d by $R_c = \rho/d$, where ρ is the electrical resistivity of the contacting material [6].

In this paper, we summarize our work on using finite element analysis (FEA) to model the electrical contact between two copper plates via a *single,* conducting, spherical, particle in an ACF. First, we will use results of classical cylindrical constriction to validate the FEA calculation by comparing the analytical expression with numerical results. Then we will use the same methodology to explore electrical contacts made with two types of spherical particles: a solid metallic particle and an insulating particle coated with an electrical conducting coating. Finally, we will use FEA and theoretical calculations to examine the electrical behavior of a contact contaminated with insulative debris.

2. Theory

We will follow the treatment given by Jones [7] to solve the Laplace's equation for the electrical potential of a cylindrical constriction.
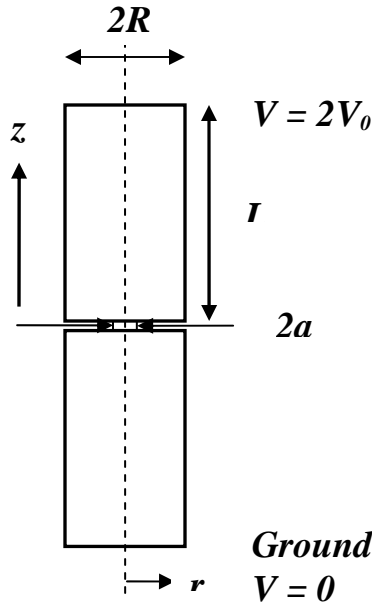
Figure 2. The constriction of radius a in a cylinder of radius R. The dashed line is the axis of symmetry. The applied potential between top and bottom of the cylinders are $2V_0$, and then by symmetry, the potential at the welded region is V_0 [8].

Consider two identical copper cylinders, welded together at the middle, as shown in Figure. 2. The length, L of one cylinder is very large compared to its radius, R. The welded area, identified as the constriction in this case, has a radius of a, and R is much larger than a ($R>>a$). The thickness of the welded joint is considered very small.

The potential V in the cylinder, which is made up of a homogeneous medium, obeys the Laplace's equation.

$$\nabla^2 V = 0 \qquad (1)$$

The above equation is solved in cylindrical coordinates with the following boundary conditions: the potential at infinity is zero; the potential at $z = 0$ is V_0; and the electric field beyond the constriction is zero (i.e., $dV/dz = 0$ at $z = 0$ with $r > a$. The current density $J(r,0)$ at the constriction is then given by,

$$J(r,0) = -\frac{1}{\rho}\frac{\partial V}{\partial z}, \quad \text{which reduces to}$$

$$J(r,0) = \frac{2V_0}{\pi\rho}\frac{1}{\sqrt{(a^2 - r^2)}} \qquad (2)$$

In Fig. 3, we show the results of FEA in comparison with the Equation (2). There is a very good agreement between the two as expected [8].
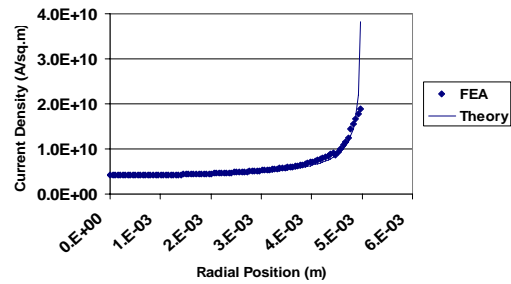

Figure 3. The comparison of finite element analysis (FEA) calculation of current density in the constriction as a function of position with the analytical expression of Equation 2 [8].

3. Pristine Contact
There are many conducting particles on a contact pad or a circuit trace when we use an ACF adhesive. However, we will examine the behaviour of a *single* conductive particle for simplicity [8]. To represent a real conductive particle participating in an electrical contact, the particle is assumed to be embedded in a pad or a circuit trace (Figure 1). We will further assume that the same metal, such as copper or silver, is used in bonding pads as well as in the conductive particle.

3.1. Solid conducting particle
We used 3D modeling in COMSOL, as shown in Figure 4, to study the electrical behavior of a conducting sphere pressed between two copper plates. We assume, for simplicity, that the adhesive medium between the plate where the silver particle is embedded is a perfect electrical insulator to form a metallurgically clean contact.

The radius of the silver sphere is taken as 20 x 10^{-6} m. The constriction, in this case, is 12 x 10^{-6} m which is the diameter of the contact

circle. The resulting current density due an applied potential of 0.1 V was studied by solving the Laplace's equation as before with the COMSOL AC/DC module, and the total current through the particle was calculated by integrating the current density across the area of the contact circle. For the expediency of calculations, only one half of the sphere was used due to the two-fold symmetry of the geometry. The total current is then obtained by doubling the calculated value.

The resistance of the sphere, determined using the total current through the sphere of radius 20×10^{-6} m, is 3.3×10^{-3} Ohm with 5738 mesh elements. For this contact the Holm's equation predicts a constriction resistance of 3.7×10^{-3} Ohm.
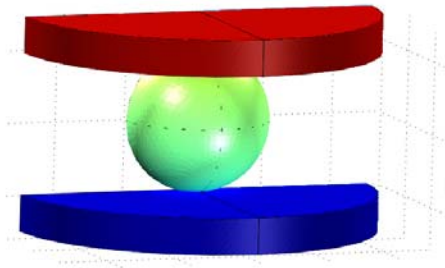

Figure 4. The 3D model used in finite element analysis (FEA) of a solid conducting sphere [8].

For the rest of the analysis of contacts with a spherical particle, we used 2-dimensional geometry of a circle as shown in Figures 5 and 6, for simplicity.
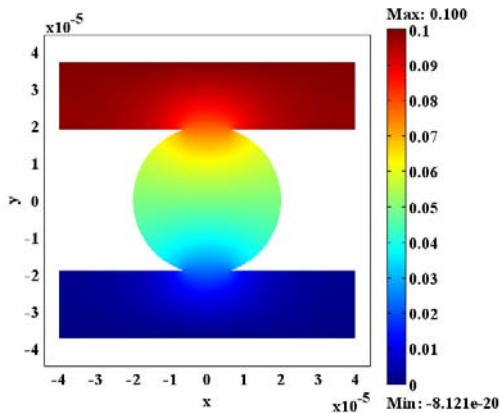

Figure 5. The distribution of the electrical potential over the conducting solid sphere with two contact plates at the top and the bottom shown in 2D [8].
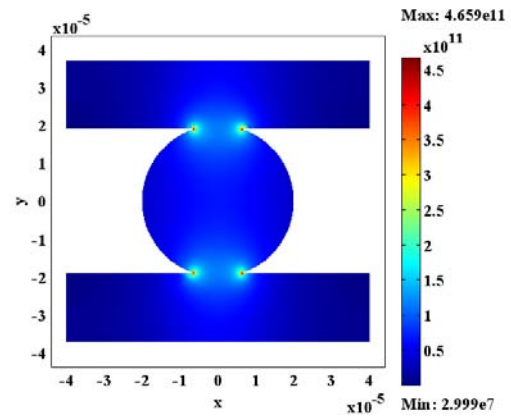

Figure 6. The calculated current density distribution in the conducting solid sphere of Figure 5 [8].

Table 1. Parameters used in finite element analysis

#	Parameter	Value	Unit
1	Diameter of sphere	40×10^{-6}	m
2	Thickness of top and bottom plates	12×10^{-6}	m
3	Conductivity of Cu	6.16×10^{7}	S/m
4	Conductivity of glass	1.0×10^{-14}	S/m
5	Indentation distance	0.7×10^{-6}	m
6	Applied voltage	0.10	V
7	Coating thickness	0.4×10^{-6}	m

The parameters in Table 1 were used in the FE analysis of the spherical particle (Figure 4). Again, the top electrode was set at an electrical potential of 0.1 V, the bottom at ground potential ($V = 0$). All other boundaries were set as electrical insulating.

Figure 6 shows the resulting current density distribution from the analysis. At the edges of the contact circles, the current density seems to be enhanced.

3.2 Coated particle

Figure 7 shows a cross sectional diagram of a silver coated glass sphere of diameter 40 micrometers making electrical contact with two copper plates as in a typical ACF bonding. Using identical conditions to that of the solid particle,

we calculated the current density. Figure 7 shows the resulting distribution of the electric potential on the coated particle while the associated current density distribution is shown in Figure 8.

A comparison plot of current density profiles of both the solid sphere and coated sphere is given in Figure 9. This clearly shows the differences of the two cases which will be discussed below.
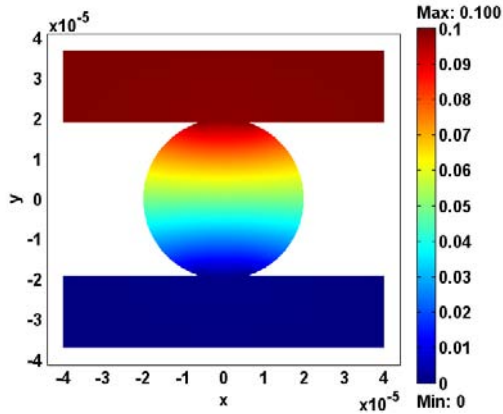

Figure 7. Silver coated glass sphere between two Cu plates: the distribution of the electrical potential across the silver coated glass sphere with an applied potential of 0.1 V between the contact plates [8].
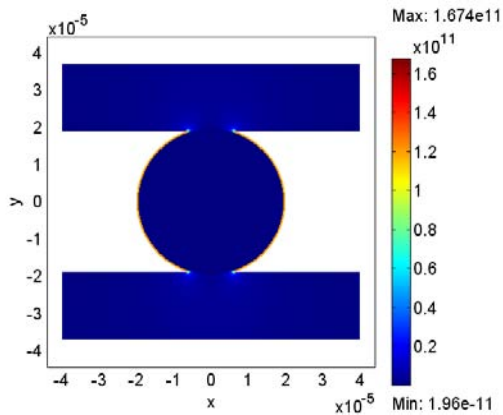

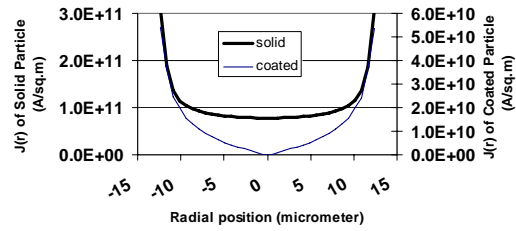Figure 8. Distribution of the current density on the silver coated glass sphere of Figure 7 [8].

Figure. 9. Comparison of the radial distribution of current density within the contact circle of a solid particle and a coated particle of same size [8].

4.   Contaminated Contact

Consider some insulative debris present within the contact circle at the interface of the bonding pad and the conducting particle (Figure 10).
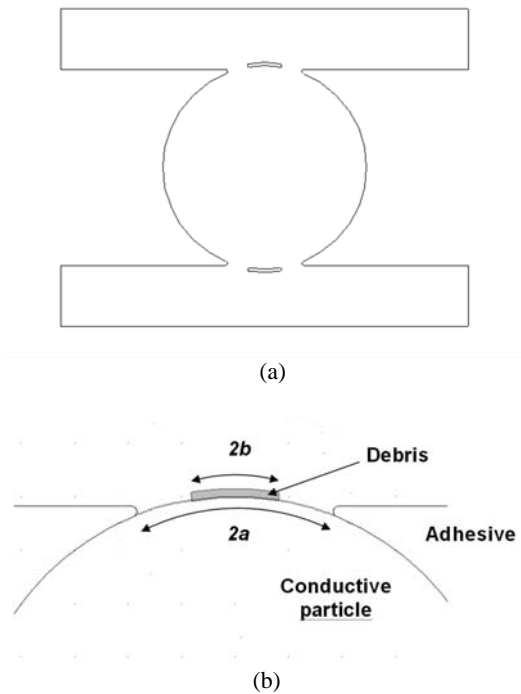

(a)

(b)

Figure 10. (a) A schematic diagram of a conductive particle with insulative debris on it. (b) An enlarged cross sectional view of the contact spot showing the dimensions a and b where $2a$ = arc length of the segment of the interface between the bonding pad and the particle and $2b$ = arc length of the debris.. The ratio $C = (b/a)^2$ is the fractional area coverage of the contact spot by debris. C is varied from zero to 90% and the corresponding contact resistance of the particle is calculated in the present work [9].

The insulative debris could be some pieces of residual adhesive left over from the flow of adhesive during bonding, or it could be some other contaminant on the bonding pads. We will consider the effect of the debris assuming they are insulating. Conductive debris, such as minute flakes of conductive coating, does not affect the resistance of the contacts dramatically.

The debris is considered to be of uniform thickness for the analysis. We assume that the extent of the contact spot is *2a,* which is the arc length of the segment of the interface between the bonding pad and the particle. Similarly, the arc length of the debris is considered as *2b* and the fractional area coverage *C* of the contact spot by debris is then given by the ratio of their areas as $(b/a)^2$ (Figure 10). We assume that the top and bottom contacts are circular plates for simplicity. The same geometrical parameters are used for both types of particles except in one case the particle is a solid metal while in the other case a glass bead is coated with a thin metal. The parameters used in the analysis are shown in Table I.

As in the pristine case, the Laplace's equation was solved for increasing values of coverage of debris *C* for two geometries: a solid particle and a coated particle.

The following boundary conditions were used: the potential of bottom plate was zero (ground); the potential of top plate was set at V_0 where V_0 is varied between 0 and 0.1*V* at intervals of 0.01*V*; and elsewhere insulating conditions were invoked.

Once V(x, y) was known the current density J(x, y) was obtained by

$$J(x, y) = -\frac{1}{\rho}\nabla V(x, y).$$

The current *I* was calculated by integrating the current density J(x, y) over an area of interest, for example, over the contact spot, or the top of the pad. The plot of current *I* vs. applied potential *V* was used to calculate the total resistance of the particle by the simple use of Ohm's law.

The coverage *C* of debris was varied from zero to about 0.90 at equal intervals for both cases and using the above procedure the resistance for each case was determined. COMSOL Multiphysics allows convenient use of parametric analysis where, for example, the applied voltage can be varied at predetermined steps for a given geometry with fixed boundary conditions.

The results of the above computations were used to observe the debris's effect on the contact resistance in both types of conducing particles and the results were compared. We derived approximate expressions for contact resistance analytically for the two cases where the debris is concentric with the contact circle and where they are non-concentric as well to further validate the behaviour seen with FEA [9].

The output of the analysis, which is the current density distribution of the particles in Figure 11 (a) and 11(b), is shown in Figure12 (a) and 12 (b), respectively. As with the constriction on clean particles, the current distribution was non-uniform around the debris.
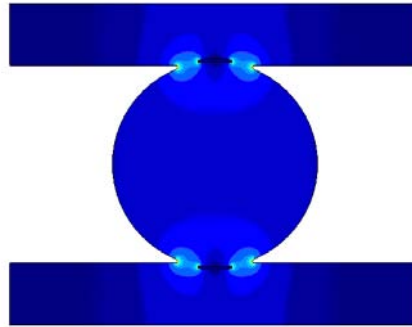

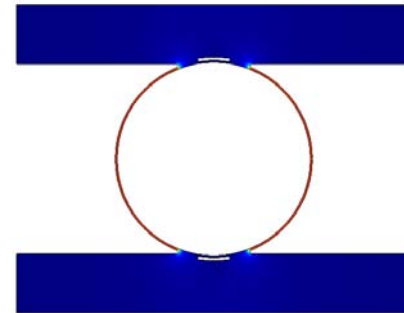Figure 11 (a). The map of current density of the contaminated solid particle with debris [9].

Figure. 11 (b). The map of current density of the contaminated coated particle [9].

The preferential conduction at the periphery of the constrictions was observed with debris. Also, the center of the contact spot of the coated particle showed no significant participation in conduction.

The results there show that, in spite of increased debris coverage, the contact resistance of the coated particle is hardly affected. We show the contact resistance normalized with respect to that of a clean particle, for both cases, in a single plot in Figure 12. Here the effect of debris is seen dramatically and it shows that coated particles are more forgiving with respect to contamination of the contact spot than the solid particle, functionally an advantage over the solid conducting particles. Theoretical predictions [9] of contact resistance agree very well with results from FEA in both cases (Figure 12).
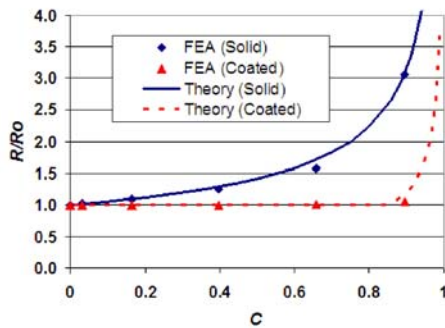

Figure. 12. Normalized contact resistance of particles as a function of coverage C of insulative debris at the contact circle. Symbols show results of FEA, while the lines show values estimated using theoretical predictions [9] (Solid line: solid conducting particle; dashed line: insulating particle with a conducting coating) [9].

5. Discussion

The solid particle can not tolerate debris coverage of the contact spot without altering the resistance while the coated particle maintains a constant resistance for overages up to 85% and even beyond that the increase in resistance is small in comparison to that of the solid particle.
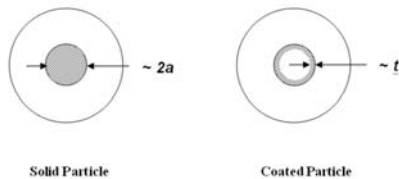

Figure. 13. Enlarged view of the contact areas of uncontaminated solid and coated particles as seen from the top or bottom of a contact. The shaded region is the area responsible for carrying current [9].

Why do these two types of particles behave so differently? The answer is evident when one examines the geometry of their respective contact spots with the conducting pad (Figure 13). We can use the concept of constriction resistance or the so-called Holm's resistance [6] to understand the above difference in resistance.

The contact resistance between a particle and a contact plane of resistivity ρ is approximately given by Holm's resistance, expressed as ρ/d, where d is the diameter of the contact spot between the two. This is valid strictly for the case when d is much less than the size of the particle representing long constriction condition [6]. In the case of a solid particle, the current is distributed over the whole contact spot which is a circle of dimension in the order of $2a$; however, in the coated particle, only an annular ring of very small width ($t \sim 2a/15$) is responsible for the flow of current due to the concentration of current density at the periphery. For example, at a typical bonding pressure of 200 psi, the indentation produced by a solid particle of diameter of 40 micron is estimated to have a contact circle about 6 micron on copper [8]. At the same time the coated sphere has a coating of thickness about 400 nm which controls the current flow. This difference makes the coated particle to have a constriction of resistance in the order of $\sim 15\rho/2a$ whereas the solid particle has a value in the order of $\sim \rho/2a$. This explains the difference in the resistance of the two types of particles.

Any debris present on the contact spot reduces the effective "aperture" (or the effective dimension d in Holm's expression) via which the current has to flow in the solid particle. However, with the coated particle, the thickness of the coating determines the contact resistance as long as the debris is contained on the contact spot such that it does not reach the ring of coating (Figure 13). Therefore, the resistance will not vary as the debris coverage is increased on the coated particle until the ring of conductive coating is reached; once the debris encroaches the ring area, a sudden increase in resistance is expected. In the solid particle, any contaminant that restricts the flow will have a larger effect on the resistance in relative terms. The finite element analysis shows this effect more quantitatively in Figure 12.

6. Conclusions

COMSOL Multiphysics has been used to analyze contact resistance of a conducting adhesive. As with cylindrical constriction, contacts between a spherical particle in a conducting adhesive and a flat conductor show non-uniform current distribution: the current is concentrated at the periphery of the contact. The radial current density distribution of solid particles and coated particles are quite different: the coated insulator particle shows that it is less sensitive to the status of the center of the contact circle.

We have also shown that a coated conducting sphere is more immune to the presence of insulative contaminants at the bonding site as compared with a solid conducting bead. Finite element analysis and theoretical calculations show a dramatic difference of contact resistance of the two cases. In practice, solid conducting particles are more expensive than their coated counterpart. The difference in electrical behavior makes an ACF made with coated particles electrically more forgiving system than that with solid particles, in addition to their economic advantage.

6. References

1. C.T. Murray, R. L. Rudman. M.B. Sabade and A.V. Pocius, Conductive Adhesives for Electronic Assemblies, *MRS Bulletin*, **28**, 449 – 454 (2003).

2. G.R. Ruschau, S. Yoshikawa, and R.E. Newnham. Resistivities of conductive composites, *J. Appl. Phys.* **72**, 953 - 959, (1992).

3. F.G. Shi, M. Abdullah, S. Chungapaiboonpatana, K. Okiyama, C. Davidson, and J.M. Adams, Electrical conduction of anisotropic conductve adhesives: effect of size distribution of filler particles, *Material Science in Semiconductor Processing*, **2**, 263 - 269 (1999).

4. L. Kogut and K. Komvopoulos, Electrical contact resistance theory for conductive rough surfaces separated by a thin insulating film, *J. Appl. Phys.* **95**, 576 - 585 (2004).

5. G. B. Dou, Y. C. Chan and Johan Liu, Electrical conduction characteristics of anisotropic conductive adhesive particles, *Journal of Electronic Packaging*. 125, 609 - 616 (2003).

6. R. Holm, *Electrical Contacts*, Springer-Verlag, 7 – 19 (1967).

7. F.L. Jones, *The Physics of Electrical Contacts.* Oxford, Clarendon Press, ch. 2 (1957).

8. R. Divigalpitiya, Electrical Characteristics of Contacts Made with Anisotropic Conductive Adhesives: Current Density Distributions at the Contacts, *IEEE Transactions on Components and Packaging Technologies*, **31**, 216 - 221 (2008).

9. R. Divigalpitiya, Effect of Insulative Debris on the Contact Resistance of Anisotropic Conductive Film (ACF) Adhesives: A Comparison between a Solid Conducting Particle and a Coated Insulative Particle, *IEEE Transactions on Components and Packaging Technologies*, **31**, 222 - 228 (2008).